

1
2
3
4
5
6
7
8
9
10
11
12
13
14
15
16
17
18
19
20
21
22
23

Supplementary information for

Principal component analysis of summertime ground site measurements in the Athabasca oil sands:

Sources of IVOCs

Travis W. Tokarek¹, Charles A. Odame-Ankrah¹, Jennifer A. Huo¹, Robert McLaren², Alex K. Y. Lee^{3, 4},
Max G. Adam⁴, Megan D. Willis⁵, Jonathan P. D. Abbatt⁵, Cristian Mihele⁶, Andrea Darlington⁶,
Richard L. Mittermeier⁶, Kevin Strawbridge⁶, Katherine L. Hayden⁶, Jason S. Olfert⁷, Elijah. G. Schnitzler⁸,
Duncan K. Brownsey¹, Faisal V. Assad¹, Gregory R. Wentworth^{5, a}, Alex G. Tevlin⁵, Douglas E. J. Worthy⁶,
Shao-Meng Li⁶, John Liggio⁶, Jeffrey R. Brook⁶, and Hans D. Osthoff^{1*}

[1] Department of Chemistry, University of Calgary, Calgary, Alberta, T2N 1N4, Canada
[2] Centre for Atmospheric Chemistry, York University, Toronto, Ontario M3J 1P3, Canada
[3] Department of Civil and Environmental Engineering, National University of Singapore, Singapore
117576, Singapore.
[4] NUS Environmental Research Institute, National University of Singapore, Singapore
[5] Department of Chemistry, University of Toronto, Toronto, Ontario, M5S 3H6, Canada
[6] Air Quality Research Division, Environment and Climate Change Canada, Toronto, Ontario, M3H 5T4,
Canada
[7] Department of Mechanical Engineering, University of Alberta, Edmonton, Alberta, T6G 1H9, Canada
[8] Department of Chemistry, University of Alberta, Edmonton, Alberta, T6G 2G2, Canada
[a] Now at: Environmental Monitoring and Science Division, Alberta Environment and Parks, Edmonton,
Alberta, T5J 5C6, Canada

* Corresponding author

25	Descriptions of instrumentation used.....	pp. 3 - 5
26	Determination of optimum PCA solution.....	pp. 6 - 11
27	Discussion of low eigenvalue components.....	pp. 10 – 16
28	Bivariate polar plots.....	pp. 17 – 18
29	Figure S-1. Scree plot.....	pg. 18
30	Table S-1. Ionimed Analytical GCU standard.....	pg. 19
31	Table S-2. The component pattern after Varimax rotation	pg. 20
32	Table S-3. The pattern after Varimax rotation with 5 components selected	pg. 21
33	Table S-4. The pattern after Varimax rotation with 6 components selected.....	pg. 22
34	Table S-5. The pattern after Varimax rotation with 7 components selected.....	pg. 23
35	Table S-6. The pattern after Varimax rotation with 8 components selected.....	pg. 24
36	Table S-7. The pattern after Varimax rotation with 9 components selected.....	pg. 25
37	Table S-8. The pattern after Varimax rotation with 11 components selected.....	pg. 26
38	Table S-9. The pattern with mixing height included after Varimax rotation with 10 components ...	pg. 27
39	Table S-10. Criteria for number of components extracted by PCA.....	pg. 28
40	Table S-11. Association of IVOCs with relevant components.....	pg. 28
41	Figure S-2. Bivariate polar plots associated with component 1.....	pg. 29
42	Figure S-3. Bivariate polar plots associated with component 2.....	pg. 30
43	Figure S-4. Bivariate polar plots associated with component 3.....	pg. 31
44	Figure S-5. Bivariate polar plots associated with component 4.....	pg. 32
45	Figure S-6. Bivariate polar plots associated with component 5.....	pg. 33
46	Figure S-7. Bivariate polar plots associated with component 6.....	pg. 34
47	Figure S-8. Bivariate polar plots associated with component 7.....	pg. 34
48	Figure S-9. Bivariate polar plots associated with component 8.....	pg. 35
49	Figure S-10. Bivariate polar plots associated with component 9.....	pg. 35
50	Figure S-11. Bivariate polar plots associated with component 10.....	pg. 36
51	References.....	pp. 36-39

52 Descriptions of instrumentation used

53 A Griffin 450 gas chromatograph equipped with a cylindrical ion trap mass spectrometer and electron
54 impact ionization (GC-ITMS) was used to quantify selected VOCs including o-xylene, decane, undecane,
55 1,2,3- and 1,2,4-trimethylbenzene (TMB), and several monoterpenes (i.e., α -pinene, β -pinene and
56 limonene). Operation, calibration and performance of this instrument have been described elsewhere
57 (Tokarek et al., 2017; Liggio et al., 2016). The GC-ITMS sampled from a 3.6 m long stainless steel inlet
58 with an o.d. of 0.635 cm from a height of 5 m above ground. A 1 m long section of the inlet was heated
59 to 110 °C and optimized to remove interference due to O₃ while avoiding decomposition of alkenes
60 (Tokarek et al., 2017). The GC oven was programmed as follows: hold at 40° C for 3.00 min, heat at 1.5°
61 C min⁻¹ to 70° C, heat at 5° C min⁻¹ to 200 °C and hold for 4 min (total 53.00 min). This was followed by a
62 5 min recovery time to allow the oven and pre-concentration trap to cool back to 40 °C. The ion trap
63 mass spectrometer was set to a *m/z* range of 50-425. After data reduction, the GC-ITMS generated 10-
64 minute average concentrations of each VOC quantified every hour.

65 During the campaign, the GC-ITMS was calibrated in the field using an IONICON VOC standard (Table S-
66 1) containing (in addition to VOCs that the GC-ITMS did not detect) α -pinene and o-xylene at mixing
67 ratios of ~ 1 ppmv and an uncertainty of 5% and 6%, respectively. A commercial calibrator assembly
68 (IONICON, GCU Standard) was used to deliver diluted calibration mixtures. The instrument responses to
69 the VOC standards were highly linear ($R^2 > 0.99$). The GC-ITMS was calibrated for other VOCs offline
70 relative to α -pinene.

71 Mixing ratios of carbon monoxide (CO), carbon dioxide (CO₂) and methane (CH₄) in ambient air were
72 quantified using a commercial cavity ring-down spectrometer (Picarro G2401) (Chen et al., 2013; Nara et
73 al., 2012). Ambient air was sampled from a height of 10 m through 0.635 cm outer diameter (o.d.)
74 perfluoroalkoxyalkane (PFA) Teflon™ tubing and a 47 mm diameter, 1 μ m pore filter at a flow rate of
75 ~0.5 L min⁻¹. A scrubber (MgClO₄) was installed at the base of the sample line to remove water from the

76 air. Operating procedures developed for Canada's greenhouse gas network of monitors across all
77 stations in Canada by the Climate Division of ECCC were followed (ECCC, 2013b).

78 The cavity ring-down spectrometer was calibrated every few days with calibrated standard gas mixtures
79 (Scott-Marrin); a target background mixture (CO₂ at a mixing ratio of 379.5 parts-per-million by volume
80 (ppmv), CH₄ at 1.976 ppmv and CO at 198.4 parts-per-billion by volume (ppbv)) and a working mixture
81 (CO₂ = 452.15 ppmv, CH₄ = 2.988 ppmv, CO = 494.5 ppbv). The estimated precision of 1 min data was
82 ±0.12 ppmv, ±0.6 ppbv, and ±1.89 ppbv for CO₂, CH₄ and CO respectively, while the estimated accuracy
83 was < 1 ppmv, < 3 ppbv, and < 4 ppbv, respectively.

84 Mixing ratios of total odd nitrogen (NO_y ≡ NO + NO₂ + ΣPAN + ΣAN + HNO₃ + HONO + 2N₂O₅ + ClNO₂ + ...)
85 were measured by a chemiluminescence analyzer equipped with a heated Molybdenum converter
86 (Thermo 42i) as described elsewhere (Tokarek et al., 2014; Odame-Ankrah, 2015).

87 The total sulfur (TS) measurements were conducted using a thermal oxidizer (Thermo Scientific Model
88 CON101) to convert TS to SO₂ and detected using a pulsed-fluorescence analyzer (Thermo Scientific,
89 Model 43iTLE). SO₂ was measured directly with a second analyzer (Thermo Scientific, Model 43iTLE).
90 Total reduced sulfur (TRS) mixing ratios were calculated by subtracting mixing ratios of SO₂ from TS.

91 Concentrations of particle-surface bound polycyclic aromatic hydrocarbons (pPAH) were measured using
92 a photoelectric aerosol sensor (EcoChem Analytics, Model PAS 2000CE) (Wilson et al., 1994; Burtscher et
93 al., 1982).

94 Two soot-particle aerosol mass spectrometers (SP-AMS, Aerodyne Research, Inc.) (Onasch et al., 2012)
95 measured non-refractory PM₁ components. Both SP-AMS were high resolution time-of-flight aerosol
96 mass spectrometers (HR-ToF-AMS) fitted with a diode pumped Nd:YAG 1064 nm laser vaporizer; one SP-
97 AMS had its oven removed to measure black carbon containing particles only using the laser. Direct
98 calibrations of rBC using mono-disperse "Regal Black" (Cabot Corp. R400) particles were carried out

99 three times during the 2013 JOSM intensive study. Positive Matrix Factorization (PMF) was performed to
100 identify the potential sources of organic aerosol as described in the companion study (Adam et al., in
101 prep). Factors associated with primary aerosol, i.e., hydrocarbon-like organic aerosol (HOA), a less
102 oxidized oxygenated organic aerosol factor (LO-OOA) and measured refractory black carbon (rBC) were
103 added as variables for PCA analysis. Mass spectra associated with LO-OOA exhibited H/C, O/C and N/C
104 ratios of ~ 1.62 , ~ 0.36 , and ~ 0.004 , respectively; while the O/C and N/C ratios are similar to HOA, the H/C
105 ratio of LO-OOA more resembles the more oxidized OOA factor (MO-OOA) (Adam et al., in prep.).

106 Particle volumes were calculated (assuming spherical particle shapes) from sub- and super-micron size
107 distributions acquired using a scanning mobility particle sizer (SMPS, TSI with a differential mobility
108 analyzer model 3081 and condensation particle counter model 3776; PM_{1}) and a 0.071 cm impactor
109 over the size range of 13.6 nm to 736.5 nm and an Aerodynamic Particle Sizer (APS, TSI 3321; PM_{10-1})
110 over the size range 1.04 μm to 10.4 μm , respectively. Both instruments were operated at ambient
111 relative humidity. The SMPS sampled through conductive silicon tubing to minimize wall losses due to
112 wall charges. The APS was operated from a container located on top of the trailer and sampled from a
113 1.6 m tall, $\frac{1}{2}$ o.d. aluminum tube whose tip was bent into a U-shape.

114 An ambient ion monitor – ion chromatograph (AIM-IC) (Markovic et al., 2012) was used to measure
115 hourly averaged gas-phase NH_3 and $PM_{2.5}$ particle-phase (i.e., of particles $< 2.5 \mu m$ diameter) NH_4^+
116 concentrations. High time-resolution particle-phase NH_4^+ measurements made by the SP-AMS were
117 scaled by interpolated phase ratios observed by AIM-IC to calculate gas-phase NH_3 concentrations at
118 high time resolution. This approach assumes the same phase ratios for $PM_{2.5}$ as for PM_{1} .

119

120 **Determination of optimum PCA solution**

121 The full component pattern (before component removal, with rotation, i.e., showing 22 components for
122 22 variables) obtained for this data set is shown in Table S-2. A common challenge in PCA is the
123 determination of the maximum number of components to retain in the analysis. Several criteria are
124 used for this purpose: the latent root criterion, where only components with eigenvalues greater than 1
125 are considered significant, the 5% variance criterion, where the last component selected accounts for
126 only a small portion (<5%) of the variance, the 95% cumulative percentage of variance criterion, where
127 the extracted components account for at least 95% of the total variance, and the Scree test. In the
128 latter, the eigenvalues are plotted against the number of components in the order of extraction (Fig. S-
129 1); to avoid including too many components with unique variance, the number of acceptable
130 components is located at the point where this plot becomes horizontal. The latent root criterion is most
131 commonly used, but tends to extract too few components when the number of variables is < 20 (Hair et
132 al., 1998). The Scree test, on the other hand, often requires "some art in administering it" (Cattell, 1966),
133 i.e., is subjective, though generally results in the inclusion of two or three more components than the
134 latent root criterion (Hair et al., 1998).

135 The maximum component number for each criterion are summarized in Table S-9. The Scree test plot
136 (Fig. S-1) shows two plateaus where the slope becomes approximately horizontal: The first is located at
137 $N = 5$ and the second at $N = 12$. The latent root criterion and the <5% variance method suggests a 7-
138 component solution, whereas the >95% percentage of variance criterion suggests using a 10-component
139 solution. Hair et al. (1998) recommend to examine component solutions with differing numbers of
140 components to evaluate which best represents the structure of the variables. In the following, solutions
141 are presented in ascending order of extracted components.

142

143

144 **5-component solution**

145 As a first attempt at interpretation of the PCA, the first cut-off of the Scree test criterion was chosen (N
146 = 5 variables). The results (after Varimax rotation) are presented in Table S-3.

147 The 5-component solution accounts for a cumulative variance of 81.0 % after rotation. Communalities
148 for the analysis, i.e., the fraction of total pollutant observations accounted for by the PCA (Otto, 2007),
149 are greater than 70% for 18 variables. The lowest communalities were obtained for gas-phase ammonia
150 (0.40), CO (0.48) and PM₁₀₋₁ (0.51). TRS and the IVOCs were also relatively poorly represented (0.63 and
151 0.73, respectively). All eigenvalues are greater than 1.

152 The component accounting for most of the variance of the data, component 1, is strongly associated
153 with all of the anthropogenic VOCs (with correlations of $r > 0.8$) and TRS ($r = 0.76$), moderately
154 associated with CH₄ ($r = 0.62$), HOA ($r = 0.44$), LO-OOA ($r = 0.59$), IVOCs ($r = 0.47$), and CO ($r = 0.53$), and
155 weakly associated with NO_y and TS ($r = 0.25$ and $r = 0.28$, respectively). Component 1 is consistent with
156 tailings ponds emissions with potentially small contributions from nearby facilities (interpreted from
157 moderate and weak correlations with rBC ($r = 0.33$) and NO_y ($r = 0.25$)), which would otherwise remain
158 unexplained. Component 2 is strongly associated with the combustion tracers NO_y ($r = 0.83$), rBC ($r =$
159 0.89) and pPAH ($r = 0.83$) and moderately associated with IVOCs ($r = 0.61$), gas-phase ammonia ($r =$
160 0.34), undecane ($r = 0.31$), and CH₄ (0.38), but weakly and not significantly with CO or CO₂ ($r = 0.19$ and
161 0.06 , respectively); this component is identified as mine fleet emissions. Component 3 is strongly
162 associated ($r > 0.9$) with the biogenic VOCs and moderately ($r = 0.55$) associated with CO₂ and is
163 identified as a biogenic component. Component 4 is strongly associated with SO₂ and TS ($r = 0.93$ and
164 0.91 , respectively) and is consistent with emissions from upgrader facilities. These four components
165 persisted, with little variation, in all solutions with a greater number of selected components (see
166 below).

167 Component 5 is strongly associated with CO₂ ($r = 0.71$), and moderately associated with PM₁₀₋₁ ($r = 0.57$),

168 CH₄ (r = 0.53) and CO (r = 0.40). We are not aware of a source type that would fit this profile, i.e.,
169 combine this particular set of pollutants without also being associated with NO_y (r = 0.02). This suggests
170 that this component is an artifact arising from an insufficient number of components used in the
171 analysis and motivates the inclusion of more components.

172

173 **6-component solution**

174 A 6-component solution is shown in Table S-4. Satisfying the percentage of variance criterion of the last
175 component accounting for less than 5% of the variance (4.6% in this case, Table S-2) was selected.

176 This solution accounts for a total variance of 85.23%. The first four components are essentially
177 unchanged from the 5-component solution (with the exception of LO-OOA in component 2 becoming
178 more weakly correlated (r = 0.22)). Component 5 is strongly associated with IVOCs (r = 0.70) and
179 moderately associated with LO-OOA (r = 0.60), and TRS (r = 0.56). Component 6 is strongly associated
180 with PM₁₀₋₁ (r = 0.81) and moderately associated with CO₂ (r = 0.62), CH₄ (r = 0.41), HOA (r = 0.30) and
181 NH₃ (r = 0.36) and, unlike the 5-component solution, not associated with CO.

182

183 **7-component solution**

184 Next, the latent root criterion gives a 7-component solution. The PCA results (after Varimax rotation) are
185 presented in Table S-5. The seven components account for a cumulative variance of 88.7% after
186 rotation. Communalities for the analysis are all greater than 60%, with the lowest communality obtained
187 for CO (0.61). All eigenvalues are greater than 1.

188 Components 1 through 4 have the same associations with similar r values as those in the 5-component
189 analysis, with the only significant exception a weaker association (r = 0.20) of component 2 with gas-
190 phase ammonia.

191 The identifications of components 5 through 7 of the 7-component solution are murky at best.

192 Component 5 is moderately associated with TRS ($r = 0.56$) and IVOCs ($r = 0.66$). Component 6 is strongly
193 associated with PM_{10-1} volume ($r = 0.89$), and moderately with CO_2 ($r = 0.54$), and CH_4 ($r = 0.36$) and
194 appears to be combination of a dust component with a source of greenhouse gases, whereas
195 component 7 is strongly associated with gas-phase ammonia ($r = 0.82$) and weakly associated with CO (r
196 $= 0.29$). Both appear to be amalgamations of distinct sources and suggest that too few components
197 were selected. Hair et al. (1998) note that the latent root criterion has a tendency to extract a
198 conservative number of components if the number of variables is < 20 , close to the 22 variables in this
199 analysis, consistent with what is observed here. Hence, the 7-component solution is sub-optimal.

200

201 **8-component solution**

202 An 8-component solution is presented in Table S-6. Not satisfying any criterion, it is included here for
203 the sake of completeness. Owing to the inclusion of an additional component, the cumulative variance
204 improved to 91.6%. The greatest improvement was seen for CO, gas-phase ammonia, as well as the
205 IVOCs, whose communalities increased from 0.61, 0.91, and 0.80 (for the 7-component solution) to 0.96,
206 0.96 and 0.84, respectively.

207 The main effect of the inclusion of an additional component was the separation of component 7 into
208 two distinct components: one of these was strongly associated with gas-phase ammonia ($r = 0.92$), and
209 the other was strongly associated with CO ($r = 0.85$). A considerable fraction of the CO observed in the
210 region is generated as a byproduct of the photochemical oxidation of hydrocarbons (Shephard et al.,
211 2015); component 8 appears to capture this source, whereas component 1 captures the anthropogenic
212 emissions. The area near the oil sands mining operations is enriched in ammonia, which originates from
213 multiple sources: it is used as a floating agent to separate and recover bitumen from tar and is
214 generated during bitumen upgrading (called hydrotreating) in which N is removed as NH_3 , and can be
215 present as a contaminant in tailing ponds. Other sources, such as agricultural activities, biological decay

216 processes, and smoldering fires are relatively minor in the region (Bytnerowicz et al., 2010). The weak
217 association of component 2 with ammonia ($r = 0.22$) may capture the use of ammonia as a floating
218 agent, whereas component 8 embodies the remaining sources.
219 Component 5 is strongly associated with IVOCs ($r = 0.71$), and moderately associated with LO-OOA($r =$
220 0.65) and TRS ($r = 0.40$). It is unclear if these variables originate from the same source or are forced
221 together as a result of having chosen too few components. Considering that component 7 is split when
222 an additional component is used (see below), the latter is more likely. Component 6 remains strongly
223 associated with PM_{10-1} volume ($r = 0.89$), and moderately associated with CO_2 ($r = 0.53$), and CH_4 ($r =$
224 0.35) and is difficult to interpret. Because of the unclear classification of components 5 through 8, the 8-
225 component solution is rejected.

226

227 **9-component solution**

228 A 9-component solution is presented in Table S-7. Components 1 through 8 describe sources that are
229 qualitatively similar to those provided by the 8-component solution. Component 9 is strongly associated
230 with TRS ($r = 0.71$) and weakly associated with o-xylene ($r = 0.30$); its profile is consistent with tailings
231 ponds emission, where the presence of naphtha as a diluent gives rise to BTEX emissions and bacteria
232 produce reduced sulfur compounds (Small et al., 2015; Warren et al., 2016). Component 6 is strongly
233 associated with PM_{10-1} ($r = 0.89$) and moderately associated with CO_2 ($r = 0.54$) and CH_4 ($r = 0.41$). We
234 have decided to reject this solution on the basis that $< 95\%$ cumulative variance is observed.

235

236 **10-component solution**

237 Next, a 10-component solution with cumulative variance of 95.5%, satisfying the 95% criterion, was
238 considered. With this solution, all communalities are >0.85 (Table 3). Component 6 is strongly associated
239 with CO_2 ($r = 0.77$) and moderately associated with CH_4 ($r = 0.59$) but is not associated with other

240 combustion tracers and is identified as inactive open-pit mines (see main text). Component 7 is strongly
241 correlated with PM_{10-1} ($r = 0.93$) and is identified as wind-blown dust. Component 8 and 9 are strongly
242 associated with a single variable each, gas-phase ammonia ($r = 0.94$) and CO ($r = 0.87$), respectively.
243 Component 10 is strongly associated with TRS ($r = 0.71$) and moderately associated with o-xylene ($r =$
244 0.32). Overall, this component is most consistent with a tailings ponds source, where the presence of
245 naphtha as diluent gives rise to BTEX emissions, and sulfur-reducing bacteria are at work (Small et al.,
246 2015; Warren et al., 2016). Overall, the 10-component solution was judged to be optimal.

247

248 **11-component solution**

249 The 11-component analysis is presented in Table S-8. Component 10 is now strongly associated with LO-
250 OOA ($r = 0.72$) and moderately with rBC ($r = 0.34$), and has a low eigenvalue of 0.87. This solution is
251 therefore rejected as we believe it contains too many components.

252

253

254 **Discussion of low-eigenvalue components**

255

256 **Component 6: A non-combustion source of CO₂ and CH₄**

257 Component 6 of the analysis has a strong association with the greenhouse gases CO₂ (r = 0.77) and a
258 moderate association with CH₄ (r = 0.59) but is not associated with tracers of combustion (i.e., NO_y,
259 pPAH, rBC) or naphtha (i.e., anthropogenic VOCs).

260 A significant amount of carbon is stored in bitumen, which, on geological time scales, conduces
261 formation of CO₂ and CH₄ (i.e., natural gas) reservoirs and pools. When bitumen is mined, substantial
262 emissions of CO₂ and, in particular, of CH₄ occur (Johnson et al., 2016). It is unclear, though, to what
263 extent these greenhouse gases are released from "hot spots" (i.e., from a small number of locations)
264 through surface cracks and fissures in the mine faces, or from new material that is exposed and then
265 releases greenhouse gases during material handling, transport and processing (Johnson et al., 2016). The
266 PCA analysis presented here would be more consistent with the "hot spots" hypothesis since
267 component 6 is not associated with NO_y, PAHs, or CO, which are expected to be emitted by the Diesel
268 machinery involved in surface mining (i.e., active disturbance of the bitumen).

269 Another potential source contribution to component 6 is the degradation of peat and surface soil.
270 Peatland soils, as they occur in the boreal forest surrounding the AMS 13 site, have long been
271 recognized as important contributors to greenhouse gas fluxes and may also be contributing to
272 component 6 (Miller et al., 2014; Gorham, 1991; Warner et al., 2017). The fixation and/or release of CO₂
273 as well as consumption and/or production of CH₄ through root, anaerobic and aerobic microbial
274 respiration are dependent on soil conditions such as water table position, temperature, soil pH, and
275 plant community composition (Yavitt et al., 2005; Oertel et al., 2016; Whalen, 2005). Emissions from
276 peat and surface soil that was stripped as part of surface mining is expected to release between

277 1.1×10^{10} and 4.7×10^{10} kg stored carbon (Rooney et al., 2012), though it is unclear on what time scale this
278 release will occur. Some of this historical peat material is used for land reclamation. However, a
279 preliminary assessment of greenhouse gas fluxes from such a site gave no indication of significant
280 emissions, at least in the short term (Nwaishi et al., 2016). The bivariate polar plot shows that
281 component 6 is associated with no particular wind direction but with relatively low wind speeds ($<$
282 1.5 m/s; Figure S-7C), consistent with a dispersed surface source. Further, when variables associated
283 with secondary processes were added to the analysis (Table 7), component 6 anticorrelates with O_x ($r = -$
284 0.41). Dry deposition is a significant O_3 and NO_2 , and therefore O_x , loss process (Wesely and Hicks, 2000;
285 Zhang et al., 2002).

286 Overall, we have too little information to constrain soil fluxes for this data set. Considering the large CH_4
287 and CO_2 concentrations observed in this study, it is more likely that anthropogenic sources dominate
288 over natural soil emissions (Thompson et al., 2017). Future field campaigns at AMS 13 would benefit
289 from N_2O measurements to constrain contributions of natural sources to greenhouse gas
290 concentrations, such as those produced by microbes in water-logged soil.

291

292 **Component 7: Wind-blown dust**

293 Component 7 is correlated with PM_{10-1} ($r = 0.93$) and, weakly, with CO_2 ($r = 0.25$), CH_4 ($r = 0.11$), HOA ($r =$
294 0.23), and LO-OOA ($r = 0.25$). In the Athabasca oil sands region, surface mining has created large
295 portions of land whose surface is void of vegetation and is covered by sand and soil particles, which are
296 readily suspended by wind and vehicle traffic. Other mining activities add to the PM_{10-1} emissions,
297 including combustion processes, tailings sands, and mine haul roads, though the contributions of each of
298 these to the overall PM_{10-1} burden is uncertain (Wang et al., 2015). Recently, Phillips-Smith et al.
299 investigated metal species found in $PM_{2.5}$ aerosol at AMS 13 and found haul road dust and soil from

300 mine faces to be important sources of PM_{2.5} (Phillips-Smith et al., 2017) and, likely, PM₁₀₋₁ as well. The
301 very weak associations of this component with CO₂ and CH₄ and lack of association with NO_y (r = 0.02)
302 suggest contributions of open mine face soil in addition to dust suspended by vehicles travelling on
303 unpaved roads.

304 The size range captured by PM₁₀₋₁ may also include bioaerosol, including bacteria, fungal spores and
305 plant pollen, which constitute the "natural" background aerosol over vegetated continental regions,
306 typically contributing a few µg m⁻³ of aerosol mass (Huffman et al., 2010). Considering the large PM₁₀₋₁
307 volumes observed in this work (Table 3), the contribution of bioaerosol is likely minor.

308

309 **Component 8: Ammonia**

310 Component 8 is a single variable component strongly associated with NH₃ (r = 0.94) but with no other
311 variables: the second largest correlation coefficient is that of rBC (r = 0.13).

312 Bytnerowicz et al. (2010) reported larger concentrations of NH₃ in the oil sands region than the
313 provincial average. More recently, Shephard et al. (2015) reported enhancements of NH₃ in the general
314 area as judged from satellite observations. Both studies hence suggest the existence of anthropogenic
315 sources, though Shephard et al. (2015) speculated that biomass burning can contribute to the ammonia
316 burden in the region. A recent modelling study by Whaley et al. (2017) estimated that around half of
317 near-surface NH₃ during the study was likely from bi-directional exchange (i.e., re-emission from soil and
318 plants).

319 In the oil sands, NH₃ is used as a floating agent for the separation and recovery of bitumen from tar,
320 during bitumen upgrading in a process called "hydrotreating", and in tailing ponds, which, on occasion,
321 have been contaminated with NH₃ to such a degree that they outgas it (Bytnerowicz et al., 2010).

322 Ammonia is also used for flue gas de-sulfurization by Syncrude; emission inventories (NPRI, 2013; ECCC,
323 2013a) suggest their fugitive emissions are the largest anthropogenic source in the region, though it is
324 not clear if all sources are accurately inventoried.

325 The lack of association of ammonia with other variables in this component and the bivariate polar plots
326 (Figure S-9) are consistent with an NH₃-specific source profile, such as fugitive emissions from one or
327 more point sources that emit independently from other activities (i.e., ammonia storage tanks) and
328 natural emissions from soil and trees.

329

330 **Component 9: Background CO from VOC oxidation**

331 Component 9 is another single variable component and strongly correlates with CO ($r = 0.87$). The
332 variables with the next largest correlation coefficients are CH₄ ($r = 0.17$), 1,2,3- and 1,2,4-TMB (both $r =$
333 0.18), and o-xylene ($r = 0.16$).

334 The conventional interpretation of CO is as a byproduct of incomplete VOC oxidation, as it is found in
335 fossil fuel combustion exhaust or in biomass burning plumes. Component 9, however, is not associated
336 with NO_y ($r = -0.08$) or CO₂ ($r = 0.05$), which rules out this conventional interpretation.

337 Recently, Marey et al. (2015) examined the spatial distribution of CO in Northern Alberta using a
338 combination of satellite and ground station data and found that most CO is derived from biomass
339 burning and the photochemical oxidation of methane and other VOCs. During the 2013 JOSM study,
340 there was no obvious (i.e., tracer) evidence for fire emissions impacting the measurements at AMS 13
341 (Phillips-Smith et al., 2017), though an impact from distant sources (such as fires located 1,000s of km
342 upwind in British Columbia or Washington State) cannot be entirely ruled out. We therefore interpret
343 component 9 as a VOC oxidation product component.

344 **Component 10: Dry tailings**

345 Component 10 is strongly associated with TRS ($r = 0.71$) and moderately with o-xylene ($r = 0.32$). There
346 are weak correlations with CH_4 ($r = 0.14$) and IVOCs ($r = 0.20$). This component is qualitatively similar to
347 component 1, in that the presence of o-xylene suggests emission of naphtha, and the presence of TRS
348 and CH_4 suggests anaerobic sulfur reducing bacteria and methanogens as they occur in tailings ponds
349 (Holowenko et al., 2000; Percy, 2013; Quagraine et al., 2005). However, the absence of correlations with
350 NO_y , rBC, and CO suggests that this source is not in spatial proximity with a continuously operating
351 combustion source. The much weaker correlations of o-xylene, CH_4 , and IVOCs than for component 1
352 suggests that this component is much more "aged", i.e., emits less naphtha and bitumen.

353 As part of the reclamation process, tailings ponds in the Alberta oil sands region are converted into
354 "composite tailings", which consist of a consolidated alkaline, saline mixture of processed sand, residual
355 bitumen, clay fines, and gypsum (CaSO_4). This mixture settles and releases water, forming shallow pools
356 of surface water (Figure 4J). Due to intensive microbial activity, composite tailings deposits are strong
357 sources of H_2S and, likely, other reduced sulfur species (Warren et al., 2016; Bradford et al., 2017).
358 Composite tailings are a source consistent with the emission profile of component 10. The association
359 with TRS is explained by its production from biological activity and the presence of IVOCs by outgassing
360 from the residual bitumen. Syncrude (the company operating closest to AMS 13) has been undertaking a
361 pilot scale wetland reclamation project in the Athabasca Oil Sands Region to allow the development of a
362 fen wetland above composite tailings (Bradford et al., 2017). Component 10 is hence interpreted as a
363 dry tailings pond component, though the confidence in this interpretation is somewhat marginal as
364 judged, for example, from the low eigenvalue of 0.74.

365

366 **Bivariate polar plots**

367 Bivariate polar plots map a surface using wind direction and wind speed and then model pollutant
368 concentrations. While PCA is good at showing the temporal distribution of sources, bivariate polar plots
369 help to show the spatial distribution of sources.

370 Figure S-2 shows a sample of variables associated with component 1. This component appears to
371 dominate when winds are from the SSE and E and of moderate wind speeds (2-3 m/s).

372 Figure S-3 shows a sample of dominant variables associated with component 2. This component appears
373 to dominate when winds are from the E at low wind speeds (1-2 m/s). The map appears to track the
374 location of the Athabasca river and highway 63, corroborating that this source is from vehicular
375 emissions.

376 Figure S-4 shows a sample of dominant variables associated with component 3. This component appears
377 to dominate when winds are stagnant and local. This is unsurprising because biogenic emissions are
378 expected to be emitted in great concentrations locally since our site is surrounded on all sides by forest.

379 Figure S-5 shows a sample of dominant variables associated with component 4 (or with component 2 in
380 the secondary processes PCA). This component appears to dominate when winds are moderate (2-3
381 m/s) and from the SE and E.

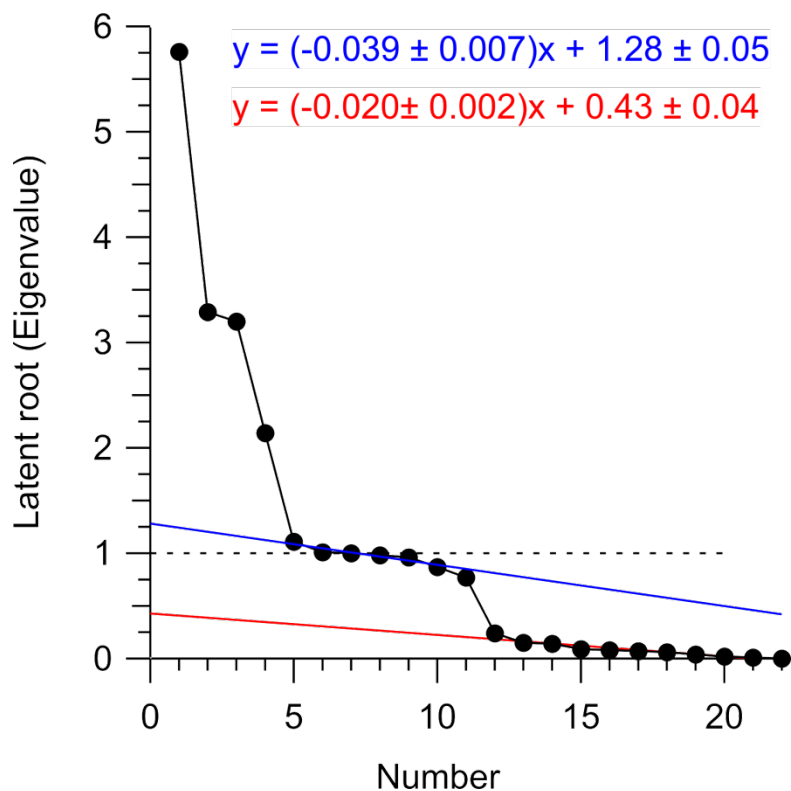
382 Figure S-6 shows a sample of dominant variables associated with component 5. This component appears
383 to dominate when winds are from the E at moderate wind speeds (2-3 m/s).

384 Figure S-7 shows a sample of dominant variables associated with component 6. This component appears
385 to dominate when winds are stagnant and local. This suggests that this source is biogenic and may be
386 due to emissions from trees.

387 Figure S-8 shows a sample of dominant variables associated with component 7. This component appears
388 to dominate when winds are from the SE and E at moderate wind speeds (1-3 m/s).

389 Figure S-9 shows a sample of dominant variables associated with component 8. This component does

390 not appear to have a specific direction associated with it and is observed in all directions. This
 391 component is observed when winds are at moderate to high speeds (2-4 m/s).
 392 Figure S-10 shows a sample of dominant variables associated with component 9. This component is
 393 observed when winds are from the S, SE, and E. This component is observed when winds are at low to
 394 moderate speeds (1-3 m/s).
 395 Figure S-11 shows a sample of dominant variables associated with component 10. This component is
 396 observed when winds are from the SSE. This component is observed when winds are around 1.5 m/s.
 397 This source is very likely a point source due to its consistency with wind direction and speed.
 398



399
 400 **Figure S-1.** Scree plot used to consider the number of components to retain. Dashed line represents the
 401 latent root criteria (eigenvalues > 1). Blue line represents the first instance of eigenvalues becoming
 402 horizontal. Red line represents the second instance of eigenvalues becoming horizontal.
 403

404 **Table S-1.** Ionimed Analytical GCU Standard..

Compound	Volume mixing ratio (ppmv)	Uncertainty (%)
Formaldehyde	1.01	±8
Methanol	1.01	±8
Acetonitrile	1.01	±6
Acetaldehyde	1.01	±5
Ethanol	1.01	±8
Acrolein	0.98	±5
Acetone	1.02	±5
Isoprene	0.99	±5
Crotonaldehyde	0.92	±6
2-Butanone	1.01	±5
Benzene	1.01	±5
Toluene	1.02	±5
o-xylene	1.03	±6
Chlorobenzene	1.02	±5
α-pinene	0.93	±5
1,2, Dichlorobenzene	1.03	±7
1,2,4-Trichlorobenzene	1.01	±9

405

406

407 **Table S-2.** The component pattern after Varimax rotation. Correlations greater than 0.30 or less than -0.30 are bolded.

	1	2	3	4	5	6	7	8	9	10	11	12	13	14	15	16	17	18	19	20	21	22
Anthropogenic VOCs																						
o-xylene	0.89	0.07	0.03	0.10	0.09	0.06	-0.03	0.11	0.15	0.06	0.26	0.11	0.00	0.04	-0.08	0.24	0.00	-0.01	-0.02	0.00	-0.01	0.00
1,2,3 - TMB	0.94	0.15	0.07	0.06	0.05	0.08	-0.01	0.06	0.17	0.01	-0.01	0.02	-0.04	0.01	-0.08	-0.14	0.03	0.00	-0.09	0.00	-0.07	0.00
1,2,4 - TMB	0.94	0.13	0.01	0.11	0.08	0.05	-0.02	0.09	0.17	0.04	0.12	0.03	-0.01	0.02	-0.06	0.03	0.01	0.00	-0.04	0.00	0.09	0.00
decane	0.91	0.22	-0.02	0.15	0.05	0.00	0.04	0.15	0.05	0.15	0.07	-0.02	0.04	-0.01	0.07	-0.03	-0.03	0.02	0.16	0.00	-0.01	0.00
undecane	0.85	0.27	-0.08	0.23	0.08	-0.03	0.06	0.05	0.00	0.20	0.01	-0.10	0.09	0.00	0.26	-0.05	-0.02	0.02	0.02	0.00	0.00	0.00
Biogenic VOCs																						
α-pinene	-0.03	-0.08	0.98	-0.11	0.02	0.05	-0.08	0.02	0.01	0.00	-0.01	0.02	0.00	0.00	-0.01	0.01	-0.08	-0.01	0.00	0.09	0.00	0.00
β-pinene	-0.02	-0.08	0.97	-0.12	0.01	0.05	-0.08	0.01	0.01	0.01	0.01	-0.02	0.00	-0.02	0.02	0.00	-0.10	0.01	0.01	-0.09	0.00	0.00
limonene	0.08	-0.02	0.92	-0.08	0.06	0.23	-0.11	0.08	0.02	0.07	-0.05	0.02	-0.03	0.03	-0.02	0.00	0.23	0.00	-0.01	0.00	0.00	0.00
Combustion tracers																						
NO _y	0.26	0.80	-0.25	0.21	0.03	-0.05	0.10	0.19	-0.04	0.07	0.04	0.01	0.34	0.00	0.04	0.00	-0.01	-0.01	0.01	0.00	0.00	0.00
rBC	0.31	0.80	0.03	0.05	0.08	0.07	0.11	0.24	0.12	0.34	-0.03	0.02	-0.02	-0.05	0.02	-0.01	0.00	0.22	0.01	0.00	0.00	0.00
CO	0.41	0.18	0.04	0.02	0.08	0.07	0.05	0.03	0.88	0.06	0.00	0.02	0.00	0.01	0.00	0.00	0.00	0.00	0.00	0.00	0.00	0.00
CO ₂	0.10	0.09	0.46	-0.12	0.23	0.82	-0.14	-0.03	0.07	0.00	-0.05	0.02	-0.01	0.01	0.00	0.00	0.00	0.00	0.00	0.00	0.00	0.00
Aerosol species																						
pPAH	0.07	0.94	-0.08	-0.11	0.02	0.06	0.14	0.00	0.09	-0.15	0.00	0.01	-0.14	-0.07	-0.02	0.00	0.00	-0.10	0.00	0.00	0.00	0.00
PM ₁₀₋₁	0.18	0.13	0.07	0.10	0.94	0.16	-0.03	0.04	0.07	0.10	0.08	0.02	0.00	0.01	0.00	0.00	0.00	0.00	0.00	0.00	0.00	0.00
HOA	0.41	0.74	0.02	0.11	0.21	0.11	-0.04	0.13	0.15	0.19	0.10	0.05	0.01	0.35	0.00	0.01	0.01	-0.01	0.00	0.00	0.00	0.00
LO-OOA	0.45	0.17	0.13	0.25	0.19	0.01	-0.04	0.28	0.10	0.73	0.16	0.02	0.01	0.03	0.01	0.00	0.00	0.00	0.00	0.00	0.00	0.00
Sulfur																						
TS	0.25	0.04	-0.16	0.94	0.07	-0.05	-0.02	0.02	0.01	0.09	0.14	0.00	0.01	0.01	0.01	0.00	0.00	0.00	0.00	0.00	0.00	0.01
SO ₂	0.11	0.02	-0.15	0.98	0.04	-0.04	-0.03	-0.02	0.01	0.05	-0.05	-0.01	0.01	0.01	0.00	0.00	0.00	0.00	0.00	0.00	0.00	-0.01
TRS	0.57	0.05	-0.08	0.11	0.14	-0.05	0.03	0.16	-0.01	0.13	0.77	0.02	0.00	0.01	0.00	0.00	0.00	0.00	0.00	0.00	0.00	0.00
Other																						
IVOCs	0.34	0.34	0.12	-0.03	0.05	-0.02	-0.02	0.84	0.04	0.18	0.13	0.01	0.01	0.01	0.00	0.00	0.00	0.00	0.00	0.00	0.00	0.00
NH ₃	0.01	0.19	-0.23	-0.04	-0.03	-0.09	0.95	-0.01	0.04	-0.01	0.01	0.00	0.01	0.00	0.00	0.00	0.00	0.00	0.00	0.00	0.00	0.00
CH ₄	0.60	0.39	0.10	-0.05	0.14	0.44	0.00	0.06	0.16	0.08	0.09	0.46	0.01	0.03	-0.02	0.01	0.00	0.00	0.00	0.00	0.00	0.00
Eigenvalues	5.76	3.29	3.20	2.14	1.11	1.01	1.00	0.98	0.96	0.87	0.77	0.24	0.15	0.14	0.09	0.08	0.07	0.06	0.04	0.02	0.01	0.00
% of variance	26.17	14.97	14.55	9.75	5.06	4.60	4.53	4.46	4.34	3.94	3.51	1.09	0.69	0.63	0.42	0.37	0.33	0.28	0.17	0.08	0.06	0.00
% cum. var.	26.17	41.14	55.69	65.43	70.49	75.09	79.62	84.07	88.42	92.36	95.87	96.97	97.66	98.29	98.71	99.08	99.41	99.69	99.86	99.94	100.0	100

409 **Table S-3.** The pattern after Varimax rotation with 5 components selected.

	1	2	3	4	5	Communalities
<u>Anthropogenic VOCs</u>						
o-xylene	0.94	0.08	0.03	0.09	0.15	0.93
1,2,3 - TMB	0.90	0.14	0.04	0.01	0.23	0.89
1,2,4 - TMB	0.95	0.14	-0.01	0.09	0.18	0.97
decane	0.91	0.27	-0.03	0.16	0.05	0.93
undecane	0.82	0.31	-0.10	0.26	0.05	0.84
<u>Biogenic VOCs</u>						
α-pinene	-0.03	-0.05	0.94	-0.15	0.04	0.91
β-pinene	-0.02	-0.06	0.94	-0.15	0.03	0.90
limonene	0.07	0.02	0.94	-0.10	0.18	0.93
<u>Combustion tracers</u>						
NO _y	0.25	0.83	-0.29	0.22	0.02	0.89
rBC	0.33	0.89	0.04	0.07	0.13	0.92
CO	0.53	0.19	-0.02	-0.08	0.40	0.48
CO ₂	0.07	0.06	0.55	-0.13	0.71	0.83
<u>Aerosol species</u>						
pPAH	0.01	0.83	-0.20	-0.20	0.27	0.84
PM ₁₀₋₁	0.21	0.19	0.15	0.29	0.57	0.51
HOA	0.44	0.75	0.03	0.15	0.32	0.88
LO-OOA	0.59	0.37	0.28	0.41	-0.06	0.74
<u>Sulfur</u>						
TS	0.28	0.04	-0.18	0.91	0.01	0.94
SO ₂	0.10	0.01	-0.18	0.93	0.05	0.91
TRS	0.76	0.10	-0.04	0.17	-0.13	0.63
<u>Other</u>						
IVOCs	0.47	0.61	0.28	0.03	-0.25	0.73
NH ₃	0.02	0.34	-0.47	-0.21	-0.14	0.40
CH ₄	0.62	0.38	0.12	-0.09	0.53	0.84
Eigenvalues	6.42	3.79	3.56	2.34	1.70	
% of variance	29.20	17.25	16.20	10.63	7.74	
Cumulative variance	29.20	46.45	62.65	73.28	81.01	

411 **Table S-4.** The pattern after Varimax rotation with 6 components selected.

	1	2	3	4	5	6	Communalities
<u>Anthropogenic VOCs</u>							
o-xylene	0.92	0.04	0.01	0.08	0.24	0.13	0.93
1,2,3 - TMB	0.94	0.16	0.08	0.07	0.06	0.05	0.92
1,2,4 - TMB	0.95	0.13	0.00	0.11	0.16	0.08	0.97
decane	0.88	0.23	-0.02	0.18	0.28	0.00	0.94
undecane	0.79	0.28	-0.09	0.29	0.25	0.00	0.85
<u>Biogenic VOCs</u>							
α -pinene	-0.02	-0.09	0.96	-0.12	0.04	0.01	0.95
β -pinene	-0.02	-0.10	0.96	-0.12	0.05	0.01	0.94
limonene	0.09	-0.01	0.95	-0.09	0.04	0.15	0.95
<u>Combustion tracers</u>							
NO _y	0.22	0.81	-0.27	0.23	0.25	0.00	0.89
rBC	0.31	0.85	0.07	0.08	0.28	0.10	0.92
CO	0.64	0.29	0.09	0.02	-0.23	0.09	0.56
CO ₂	0.17	0.12	0.57	-0.17	-0.23	0.62	0.84
<u>Aerosol species</u>							
pPAH	0.09	0.90	-0.10	-0.14	-0.10	0.05	0.87
PM ₁₀₋₁	0.19	0.14	0.03	0.12	0.17	0.81	0.76
HOA	0.44	0.73	0.04	0.13	0.22	0.30	0.88
LO-OOA	0.46	0.22	0.17	0.32	0.60	0.21	0.79
<u>Sulfur</u>							
TS	0.25	0.02	-0.18	0.92	0.12	0.06	0.97
SO ₂	0.10	0.03	-0.15	0.97	-0.02	0.02	0.98
TRS	0.62	-0.04	-0.17	0.06	0.56	0.14	0.75
<u>Other</u>							
IVOCs	0.31	0.43	0.17	-0.06	0.70	0.02	0.80
NH ₃	0.06	0.41	-0.36	-0.11	-0.11	-0.36	0.46
CH ₄	0.68	0.42	0.15	-0.10	0.00	0.41	0.84
Eigenvalues	6.09	3.60	3.47	2.25	1.76	1.58	
% of variance	27.70	16.38	15.78	10.22	7.98	7.18	
Cumulative variance	27.70	44.07	59.85	70.08	78.06	85.23	

412

413 **Table S-5.** The pattern after Varimax rotation with 7 components selected.

	1	2	3	4	5	6	7	Communalities
<u>Anthropogenic VOCs</u>								
o-xylene	0.93	0.07	0.01	0.08	0.21	0.12	-0.05	0.93
1,2,3 - TMB	0.94	0.18	0.08	0.06	0.03	0.03	-0.03	0.93
1,2,4 - TMB	0.96	0.15	0.00	0.11	0.14	0.07	-0.02	0.98
decane	0.88	0.26	-0.02	0.18	0.26	0.00	0.01	0.94
undecane	0.79	0.30	-0.09	0.28	0.23	0.00	0.03	0.85
<u>Biogenic VOCs</u>								
α -pinene	-0.03	-0.09	0.96	-0.11	0.04	0.00	-0.05	0.96
β -pinene	-0.02	-0.10	0.96	-0.11	0.06	0.01	-0.05	0.95
limonene	0.09	0.01	0.95	-0.08	0.03	0.12	-0.13	0.95
<u>Combustion tracers</u>								
NO _y	0.22	0.83	-0.28	0.22	0.20	-0.02	0.06	0.91
rBC	0.31	0.85	0.07	0.08	0.25	0.11	0.13	0.92
CO	0.62	0.22	0.13	0.03	-0.21	0.19	0.29	0.61
CO ₂	0.17	0.17	0.56	-0.18	-0.28	0.54	-0.27	0.84
<u>Aerosol species</u>								
pPAH	0.08	0.89	-0.10	-0.15	-0.14	0.03	0.15	0.88
PM ₁₀₋₁	0.18	0.12	0.06	0.13	0.18	0.89	0.01	0.89
HOA	0.44	0.76	0.03	0.12	0.16	0.27	-0.03	0.89
LO-OOA	0.46	0.23	0.18	0.33	0.59	0.25	0.01	0.81
<u>Sulfur</u>								
TS	0.25	0.04	-0.18	0.92	0.12	0.06	-0.02	0.97
SO ₂	0.10	0.04	-0.15	0.97	-0.02	0.02	-0.03	0.98
TRS	0.62	-0.03	-0.16	0.07	0.56	0.19	0.02	0.77
<u>Other</u>								
IVOCs	0.32	0.48	0.16	-0.07	0.66	0.00	-0.05	0.80
NH ₃	0.01	0.20	-0.26	-0.06	0.00	-0.05	0.89	0.91
CH ₄	0.68	0.45	0.15	-0.11	-0.05	0.36	-0.10	0.85
Eigenvalues	6.09	3.65	3.42	2.23	1.61	1.46	1.03	
% of variance	27.70	16.60	15.57	10.14	7.33	6.66	4.70	
Cumulative variance	27.70	44.30	59.86	70.01	77.34	84.00	88.70	

414 **Table S-6.** The pattern after Varimax rotation with 8 components selected.

	1	2	3	4	5	6	7	8	Communalities
<u>Anthropogenic VOCs</u>									
o-xylene	0.93	0.08	0.03	0.07	0.14	0.13	-0.03	0.11	0.93
1,2,3 - TMB	0.91	0.19	0.09	0.06	-0.01	0.02	-0.04	0.21	0.93
1,2,4 - TMB	0.95	0.16	0.01	0.11	0.09	0.07	-0.03	0.18	0.98
decane	0.90	0.26	-0.01	0.17	0.19	0.01	0.03	0.08	0.95
undecane	0.82	0.30	-0.07	0.28	0.15	0.01	0.06	0.03	0.87
<u>Biogenic VOCs</u>									
α-pinene	-0.04	-0.10	0.97	-0.11	0.06	0.00	-0.05	0.00	0.96
β-pinene	-0.02	-0.10	0.96	-0.11	0.06	0.00	-0.04	-0.01	0.96
limonene	0.07	0.00	0.95	-0.08	0.06	0.11	-0.14	0.05	0.95
<u>Combustion tracers</u>									
NO _y	0.25	0.83	-0.26	0.22	0.19	-0.01	0.10	-0.08	0.92
rBC	0.28	0.83	0.06	0.07	0.33	0.10	0.09	0.17	0.93
CO	0.42	0.18	0.04	0.01	0.07	0.11	0.06	0.85	0.96
CO ₂	0.13	0.19	0.58	-0.17	-0.28	0.53	-0.27	0.10	0.86
<u>Aerosol species</u>									
pPAH	0.06	0.91	-0.08	-0.14	-0.11	0.03	0.16	0.06	0.89
PM ₁₀₋₁	0.18	0.12	0.07	0.12	0.16	0.89	0.01	0.06	0.89
HOA	0.42	0.75	0.03	0.12	0.21	0.26	-0.06	0.15	0.89
LO-OOA	0.46	0.19	0.15	0.30	0.65	0.24	-0.04	0.15	0.87
<u>Sulfur</u>									
TS	0.28	0.03	-0.18	0.92	0.09	0.07	-0.01	-0.02	0.97
SO ₂	0.11	0.04	-0.15	0.97	-0.01	0.02	-0.04	0.03	0.98
TRS	0.72	-0.03	-0.13	0.06	0.40	0.23	0.11	-0.20	0.80
<u>Other</u>									
IVOCs	0.35	0.43	0.13	-0.09	0.71	0.00	-0.07	0.01	0.84
NH ₃	0.01	0.22	-0.24	-0.05	-0.05	-0.04	0.92	0.05	0.96
CH ₄	0.65	0.47	0.17	-0.11	-0.08	0.35	-0.10	0.16	0.86
Eigenvalues	5.99	3.58	3.40	2.20	1.52	1.43	1.03	1.00	
% of variance	27.23	16.28	15.44	10.01	6.90	6.52	4.70	4.53	
Cumulative variance	27.23	43.51	58.95	68.96	75.86	82.37	87.08	91.61	

416 **Table S-7.** The pattern after Varimax rotation with 9 components selected.

	1	2	3	4	5	6	7	8	9	Communalities
<u>Anthropogenic VOCs</u>										
o-xylene	0.89	0.09	0.03	0.09	0.11	0.11	-0.05	0.16	0.30	0.95
1,2,3 - TMB	0.93	0.16	0.08	0.05	0.05	0.05	-0.02	0.17	-0.02	0.94
1,2,4 - TMB	0.94	0.15	0.01	0.11	0.11	0.08	-0.02	0.18	0.12	0.98
decane	0.91	0.22	-0.03	0.16	0.25	0.04	0.05	0.03	0.03	0.97
undecane	0.85	0.25	-0.10	0.25	0.24	0.06	0.10	-0.05	-0.08	0.94
<u>Biogenic VOCs</u>										
α-pinene	-0.04	-0.09	0.97	-0.10	0.05	0.00	-0.06	0.02	0.02	0.97
β-pinene	-0.03	-0.10	0.97	-0.11	0.05	0.00	-0.05	0.00	0.02	0.96
limonene	0.09	-0.01	0.94	-0.09	0.08	0.13	-0.13	0.03	-0.06	0.95
<u>Combustion tracers</u>										
NO _y	0.26	0.82	-0.26	0.22	0.22	0.00	0.11	-0.09	0.02	0.92
rBC	0.31	0.79	0.04	0.05	0.41	0.12	0.12	0.12	-0.10	0.94
CO	0.42	0.19	0.05	0.02	0.08	0.10	0.06	0.87	-0.02	0.98
CO ₂	0.16	0.17	0.56	-0.18	-0.22	0.56	-0.25	0.06	-0.17	0.86
<u>Aerosol species</u>										
pPAH	0.06	0.93	-0.07	-0.12	-0.11	0.01	0.14	0.09	0.03	0.93
PM ₁₀₋₁	0.16	0.11	0.06	0.12	0.17	0.89	0.02	0.06	0.10	0.89
HOA	0.41	0.75	0.03	0.13	0.23	0.25	-0.06	0.16	0.08	0.90
LO-OOA	0.46	0.14	0.13	0.28	0.70	0.26	-0.01	0.10	0.05	0.90
<u>Sulfur</u>										
TS	0.25	0.04	-0.17	0.93	0.08	0.06	-0.02	0.00	0.13	0.99
SO ₂	0.11	0.03	-0.15	0.97	0.01	0.02	-0.03	0.01	-0.05	0.99
TRS	0.59	0.05	-0.09	0.11	0.24	0.14	0.04	-0.04	0.71	0.96
<u>Other</u>										
IVOCs	0.32	0.41	0.12	-0.09	0.70	-0.01	-0.08	0.02	0.20	0.84
NH ₃	0.01	0.21	-0.24	-0.05	-0.04	-0.04	0.93	0.04	0.01	0.97
CH ₄	0.65	0.47	0.16	-0.10	-0.06	0.36	-0.10	0.17	0.07	0.86
Eigenvalues	5.84	3.44	3.37	2.19	1.58	1.47	1.03	0.95	0.74	
% of variance	26.54	15.63	15.30	9.98	7.19	6.66	4.69	4.31	3.38	
Cumulative variance	26.54	42.17	57.47	67.44	74.63	81.29	85.98	90.29	93.67	

418 **Table S-8.** The factor pattern after Varimax rotation with 11 factors selected.

	Factor 1	Factor 2	Factor 3	Factor 4	Factor 5	Factor 6	Factor 7	Factor 8	Factor 9	Factor 10	Factor 11	Communi- nalities
<u>Anthropogenic VOCs</u>												
o-xylene	0.88	0.08	0.03	0.10	0.13	0.07	-0.04	0.17	0.11	0.04	0.32	0.95
1,2,3 - TMB	0.94	0.16	0.07	0.05	0.11	0.05	-0.01	0.18	0.06	-0.01	-0.02	0.96
1,2,4 - TMB	0.94	0.15	0.01	0.11	0.08	0.08	-0.02	0.18	0.09	0.03	0.13	0.99
decane	0.92	0.24	-0.02	0.15	0.00	0.05	0.04	0.04	0.13	0.16	0.05	0.97
undecane	0.87	0.29	-0.08	0.22	-0.06	0.09	0.05	-0.05	0.03	0.22	-0.05	0.96
<u>Biogenic VOCs</u>												
α -pinene	-0.03	-0.08	0.98	-0.11	0.04	0.01	-0.08	0.02	0.02	0.00	0.00	0.98
β -pinene	-0.02	-0.08	0.98	-0.12	0.02	0.02	-0.07	0.00	0.00	0.02	0.01	0.98
limonene	0.08	-0.02	0.93	-0.08	0.24	0.05	-0.11	0.03	0.09	0.06	-0.05	0.95
<u>Combustion tracers</u>												
NO _y	0.27	0.83	-0.26	0.21	-0.04	0.03	0.10	-0.08	0.18	0.07	0.01	0.92
rBC	0.30	0.81	0.04	0.04	0.09	0.07	0.12	0.12	0.23	0.34	-0.05	0.95
CO	0.41	0.19	0.04	0.02	0.08	0.08	0.05	0.87	0.03	0.06	-0.01	0.99
CO ₂	0.09	0.08	0.48	-0.12	0.77	0.25	-0.14	0.05	-0.04	-0.01	-0.09	0.95
<u>Aerosol species</u>												
pPAH	0.06	0.93	-0.07	-0.12	0.07	0.02	0.14	0.10	-0.02	-0.20	0.01	0.95
PM ₁₀₋₁	0.18	0.14	0.08	0.10	0.17	0.94	-0.03	0.07	0.04	0.09	0.08	1.00
HOA	0.40	0.77	0.03	0.11	0.14	0.20	-0.07	0.16	0.09	0.19	0.13	0.92
LO-OOA	0.45	0.19	0.13	0.25	0.03	0.19	-0.04	0.11	0.27	0.72	0.16	0.98
<u>Sulfur</u>												
TS	0.26	0.05	-0.16	0.93	-0.05	0.07	-0.02	0.01	0.02	0.08	0.13	0.26
SO ₂	0.12	0.03	-0.15	0.98	-0.04	0.04	-0.03	0.01	-0.02	0.05	-0.05	0.12
TRS	0.58	0.06	-0.08	0.10	-0.04	0.14	0.03	-0.03	0.16	0.13	0.74	0.58
<u>Other</u>												
IVOCs	0.34	0.37	0.13	-0.03	-0.01	0.05	-0.03	0.03	0.82	0.18	0.12	1.00
NH ₃	0.01	0.20	-0.24	-0.04	-0.08	-0.03	0.94	0.04	-0.02	-0.01	0.01	1.00
CH ₄	0.59	0.40	0.10	-0.06	0.59	0.10	0.00	0.17	0.05	0.07	0.15	0.93
Eigenvalues	5.75	3.43	3.24	2.13	1.12	1.10	0.99	0.96	0.93	0.87	0.79	
% var.	26.14	15.61	14.72	9.66	5.11	4.99	4.51	4.35	4.22	3.95	3.60	
% Cum. var.	26.14	41.74	56.46	66.12	71.23	76.22	80.73	85.09	89.31	93.26	96.86	

419 **Table S-9.** The pattern with mixing height included after Varimax rotation with 10 components.

	1	2	3	4	5	6	7	8	9	10	Communi- nalities
<u>Anthropogenic VOCs</u>											
o-xylene	0.89	0.04	0.03	0.10	0.29	0.10	-0.01	-0.06	0.17	0.16	0.95
1,2,3 - TMB	0.94	0.17	0.10	0.04	-0.04	0.01	-0.03	-0.04	0.17	0.06	0.95
1,2,4 - TMB	0.94	0.13	0.03	0.10	0.11	0.09	-0.02	-0.06	0.18	0.07	0.98
decane	0.92	0.25	0.03	0.15	0.11	0.11	0.01	0.04	0.03	-0.04	0.97
undecane	0.87	0.31	-0.05	0.23	-0.03	0.17	0.03	0.10	-0.05	-0.11	0.96
<u>Biogenic VOCs</u>											
α -pinene	-0.02	-0.08	0.96	-0.10	0.03	0.01	-0.05	-0.11	0.01	0.02	0.96
β -pinene	-0.01	-0.08	0.96	-0.11	0.04	0.02	-0.05	-0.12	-0.01	0.02	0.96
limonene	0.11	0.02	0.95	-0.08	0.04	0.02	-0.11	-0.06	0.03	0.12	0.96
<u>Combustion tracers</u>											
NO _y	0.21	0.86	-0.25	0.21	0.11	0.06	0.10	0.01	-0.08	-0.02	0.92
rBC	0.29	0.89	0.12	0.02	0.10	0.19	0.03	0.09	0.10	-0.01	0.95
CO	0.43	0.20	0.04	0.01	0.00	0.08	0.02	0.05	0.86	0.07	0.98
CO ₂	0.15	0.17	0.56	-0.13	-0.12	0.13	-0.14	-0.12	0.08	0.68	0.91
<u>Aerosol species</u>											
pPAH	0.01	0.86	-0.09	-0.13	-0.08	-0.03	0.23	-0.18	0.12	0.17	0.90
PM ₁₀₋₁	0.31	0.22	0.05	0.15	0.12	0.88	0.04	-0.01	0.08	0.10	0.97
HOA	0.45	0.79	0.02	0.14	0.16	0.15	-0.02	-0.02	0.16	0.10	0.93
LO-OOA	0.52	0.30	0.21	0.26	0.37	0.36	-0.17	0.27	0.04	-0.18	0.88
<u>Sulfur</u>											
TS	0.27	0.06	-0.16	0.93	0.10	0.10	-0.03	0.04	-0.01	-0.02	1.00
SO ₂	0.11	0.05	-0.14	0.97	-0.06	0.06	-0.05	0.05	0.01	-0.05	0.99
TRS	0.64	0.01	-0.12	0.11	0.63	0.20	0.09	-0.04	-0.09	0.12	0.91
<u>Other</u>											
IVOCs	0.28	0.50	0.22	-0.07	0.66	0.08	-0.13	0.04	0.06	-0.18	0.87
NH ₃	0.00	0.22	-0.20	-0.07	-0.03	0.03	0.92	0.11	0.02	-0.06	0.96
CH ₄	0.64	0.43	0.15	-0.07	0.09	0.10	0.00	-0.07	0.17	0.50	0.92
Mixing height	-0.04	-0.07	-0.35	0.07	0.01	0.00	0.12	0.90	0.04	-0.07	0.96
Eigenvalues	6.06	3.81	3.51	2.16	1.19	1.12	1.03	1.02	0.94	0.92	
% var.	26.35	16.57	15.27	9.39	5.19	4.86	4.48	4.42	4.08	3.98	
% Cum. var.	26.35	42.92	58.19	67.58	72.77	77.63	82.11	86.53	90.61	94.60	

420

421

422 **Table S-10.** Criteria for number of components extracted by PCA.

Criterion	Number of components extracted	% Variance explained (after rotation)
Scree test 1	5	81.0%
< 5% variance	6	85.2%
Latent root	7	88.7%
≥ 95% cumulative variance	10	95.5%
Scree test 2	11	96.9%

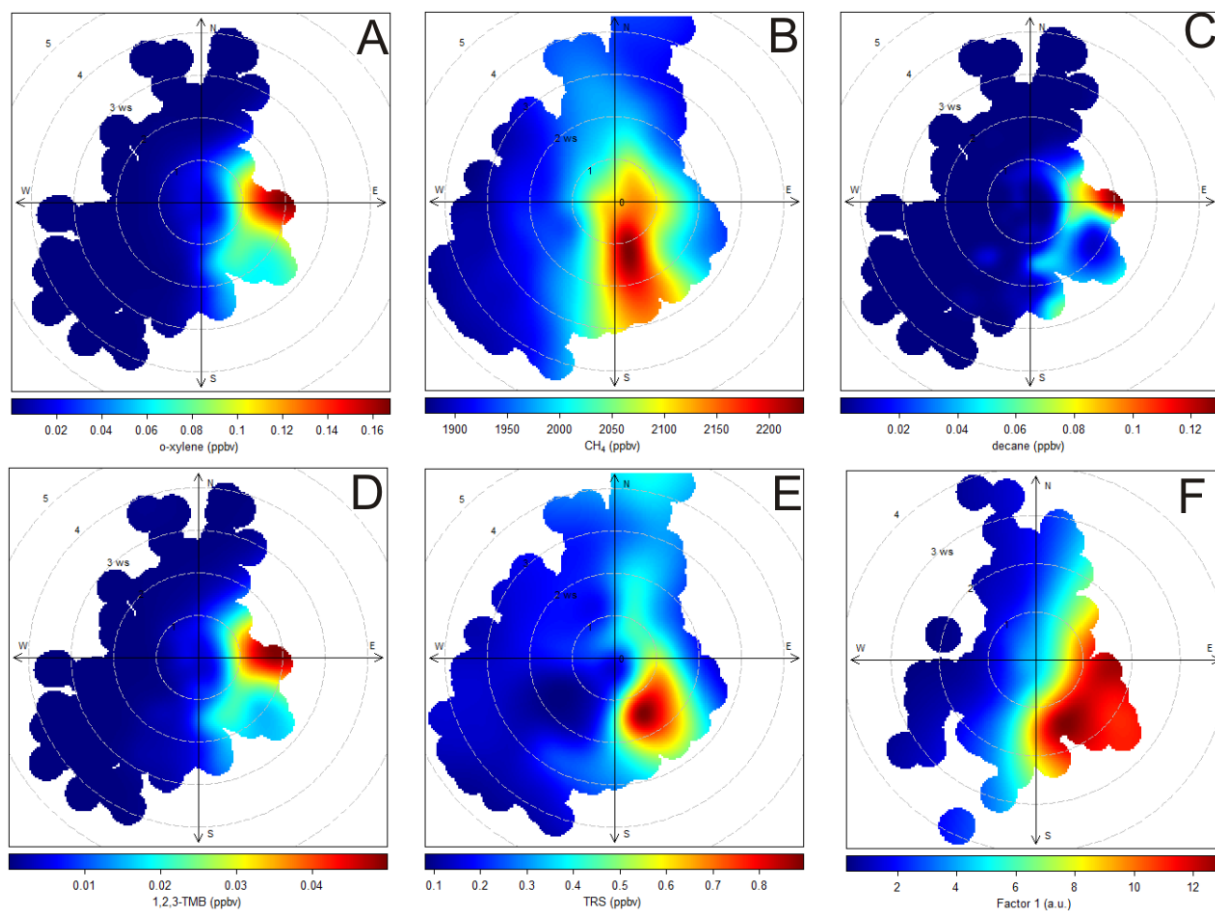
423

424

425 **Table S-11.** Association of IVOCs with relevant components.

# of components in solution	Oil sands surface mining facilities (Component 1)	Mine fleet and operations (Component 2)	Mine face (Component 5)
5	0.47	0.61	n/a
6	0.31	0.43	n/a
7	0.32	0.48	0.66
8	0.35	0.43	0.71
9	0.32	0.41	0.70
10	0.31	0.39	0.74
11	0.34	0.37	n/a

426



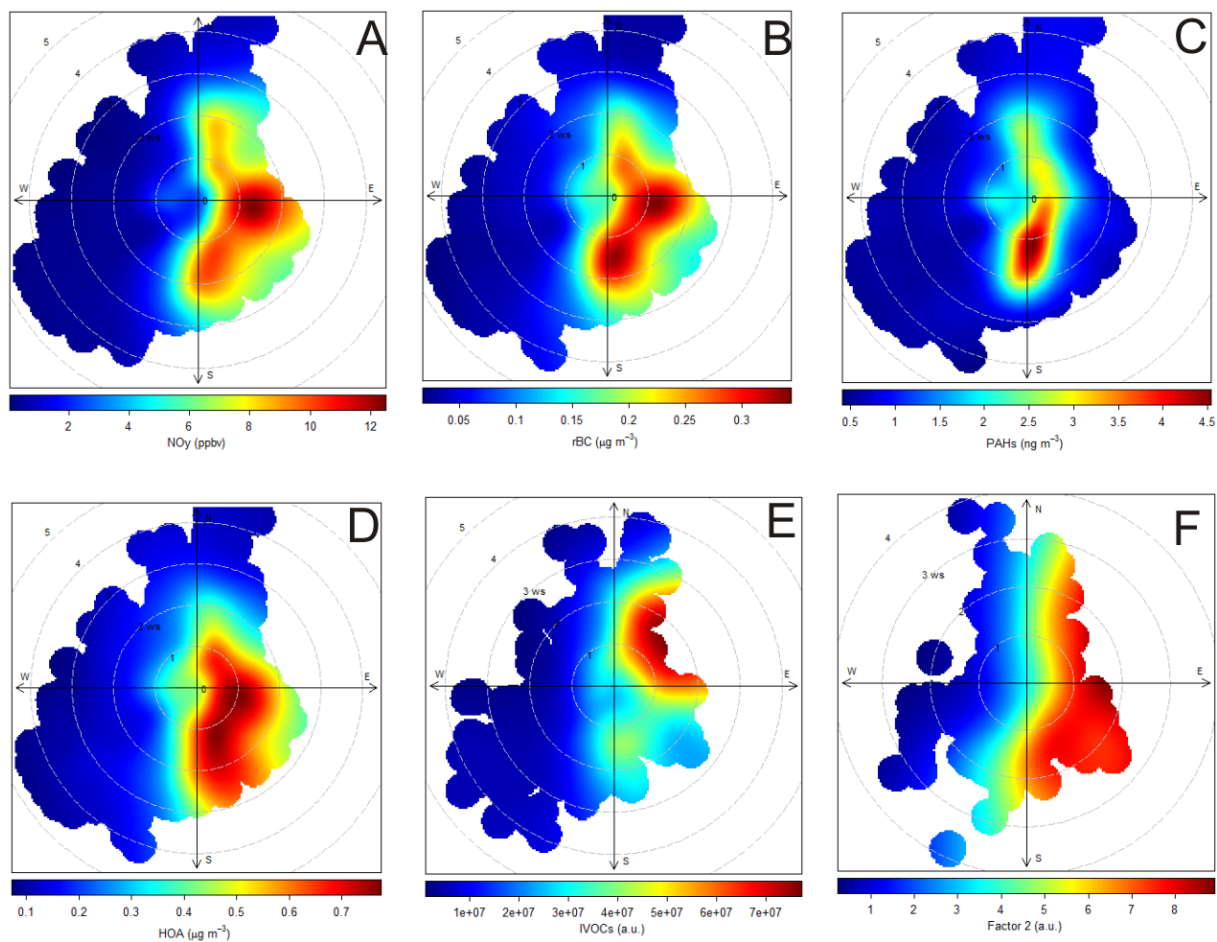
427

428 **Figure S-2.** Bivariate polar plots associated with component 1 for the optimum primary pollutant

429 solution (Table 4.). **(A)** o-xylene, **(B)** CH₄, **(C)** decane, **(D)** 1, 2, 3-TMB, **(E)** TRS, **(F)** and component 1.

430

431

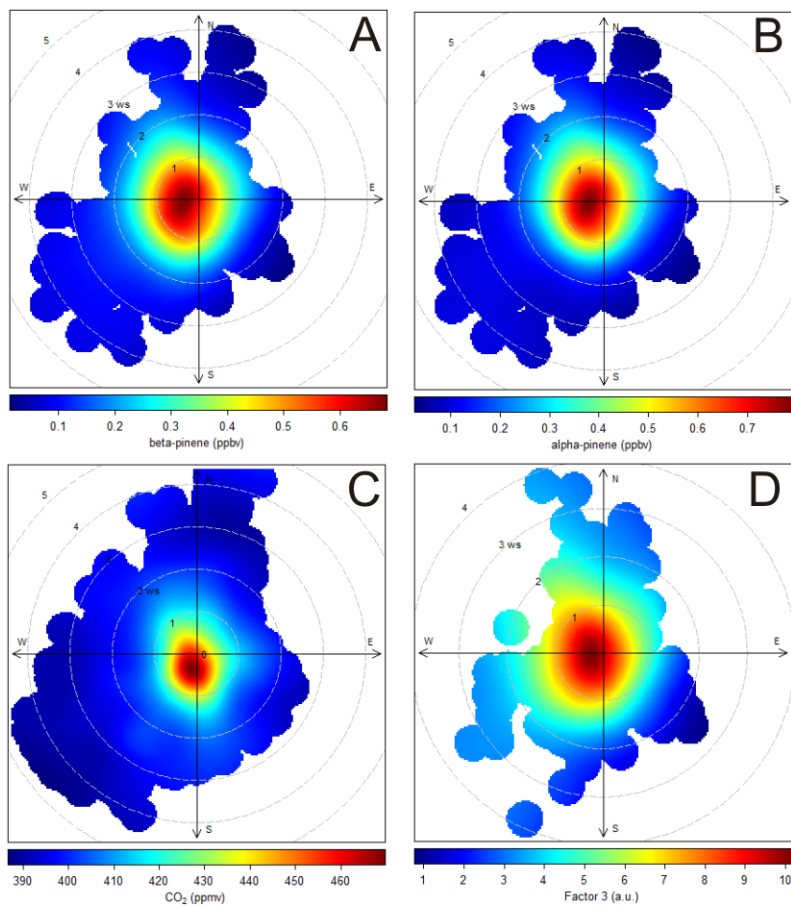


432

433 **Figure S-3.** Bivariate polar plots associated with component 2 for the optimum primary pollutant
434 solution (Table 4.). (A) NO_y, (B) rBC, (C) PAHs, (D) HOA, (E) IVOCs, (F) and component 2.

435

436



437

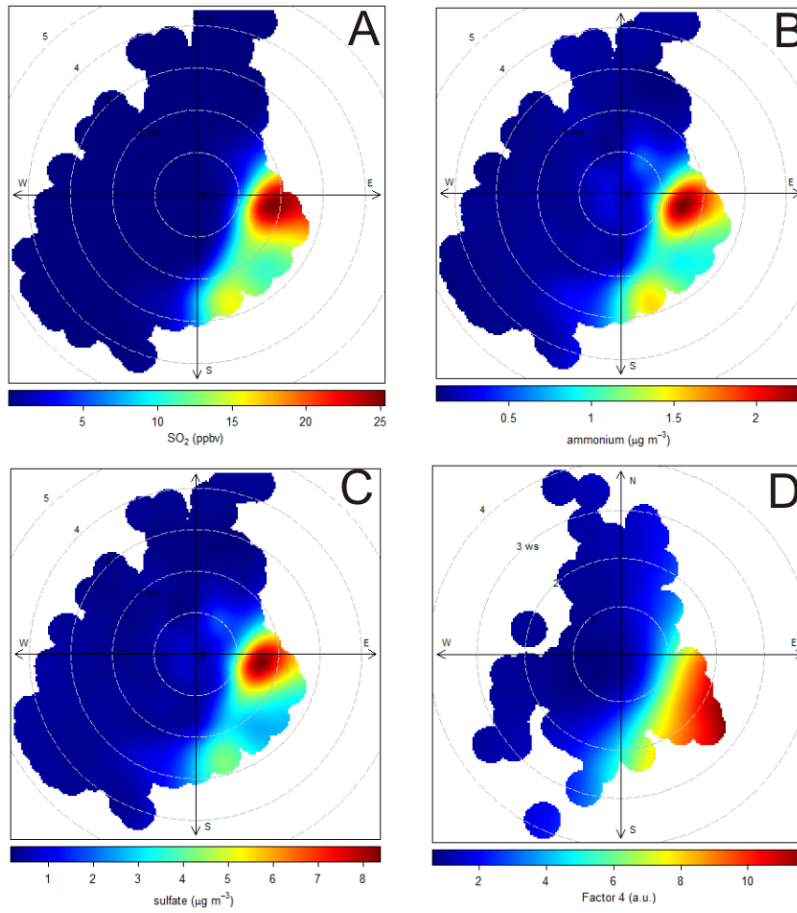
438 **Figure S-4.** Bivariate polar plots associated with component 3 for the optimum primary pollutant

439 solution (Table 4.). **(A)** β -pinene, **(B)** α -pinene, **(C)** CO₂, **(D)** and component 3.

440

441

442

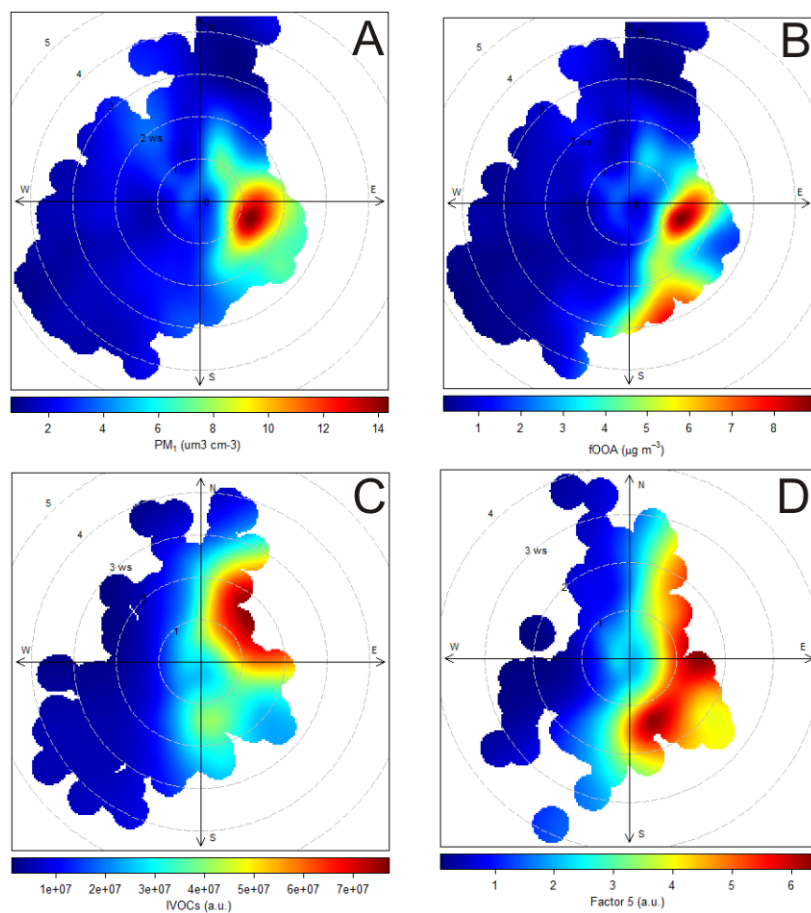


443

444 **Figure S-5.** Bivariate polar plots associated with component 4 for the optimum primary pollutant
445 solution (Table 4). **(A)** SO₂, **(B)** NH₄⁺_(p), **(C)** SO₄²⁻_(p), **(D)** and component 4.

446

447



448

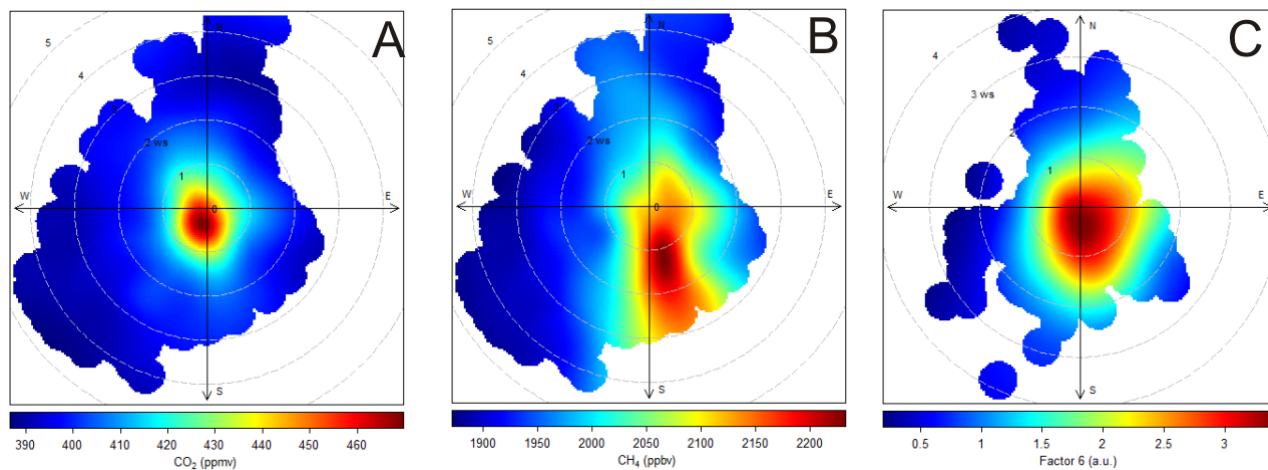
449

450

451

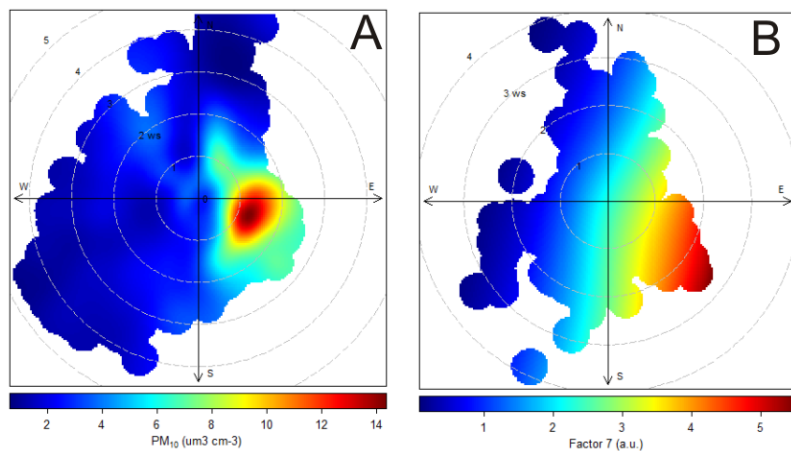
Figure S-6. Bivariate polar plots associated with component 5 for the optimum primary pollutant solution (Table 4.). **(A)** PM₁ (11-component solution), **(B)** LO-OOA, **(C)** IVOCs, and **(D)** component 5.

452
453



454
455
456
457
458

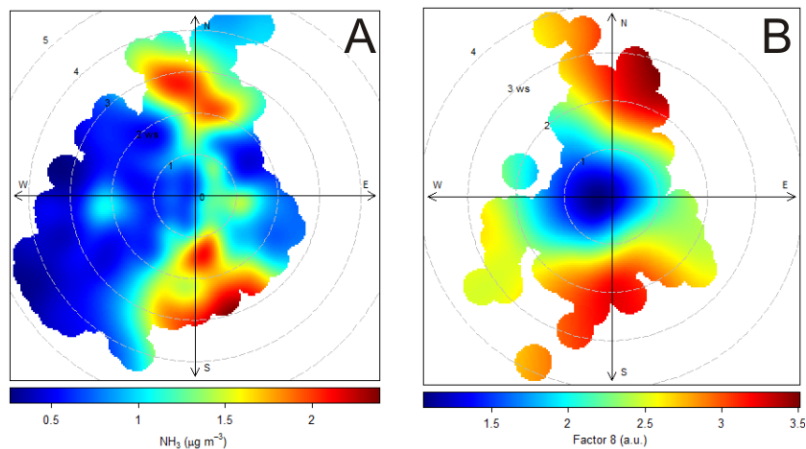
Figure S-7. Bivariate polar plots associated with component 6 for the optimum primary pollutant solution (Table 4.). **(A)** CO₂, **(B)** CH₄, and **(C)** component 6.



459
460
461
462

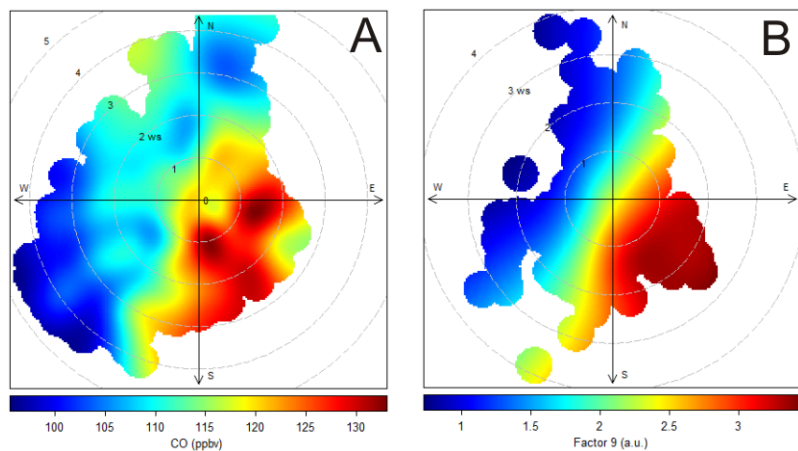
Figure S-8. Bivariate polar plots associated with component 7 for the optimum primary pollutant solution (Table 4.). **(A)** PM₁₀₋₁, **(B)** and component 7.

463
464



465
466 **Figure S-9.** Bivariate polar plots associated with component 8 for the optimum primary pollutant
467 solution (Table 4.). **(A)** NH₃, **(B)** and component 8.

468
469

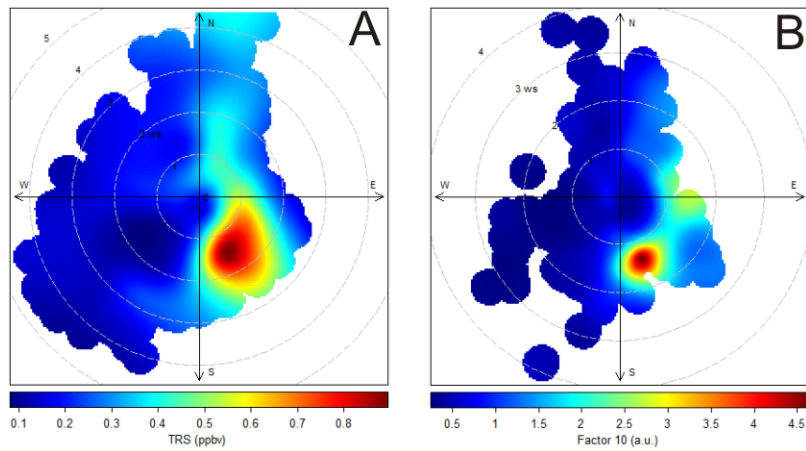


470
471 **Figure S-10.** Bivariate polar plots associated with component 9 for the optimum primary pollutant
472 solution (Table 4.). **(A)** CO, and **(B)** component 9.

473

474

475



476

477 **Figure S-11.** Bivariate polar plots associated with component 10 for the optimum primary pollutant

478 solution (Table 4.). **(A)** TRS, **(B)** and component 10.

479

480 **References**

- 481
- 482 Bradford, L. M., Ziolkowski, L. A., Goad, C., Warren, L. A., and Slater, G. F.: Elucidating carbon sources
483 driving microbial metabolism during oil sands reclamation, *Journal of Environmental Management*,
484 188, 246-254, 10.1016/j.jenvman.2016.11.029, 2017.
- 485 Burtscher, H., Scherrer, L., Siegmann, H. C., Schmidtott, A., and Federer, B.: Probing aerosols by
486 photoelectric charging, *J. Appl. Phys.*, 53, 3787-3791, 10.1063/1.331120, 1982.
- 487 Bytnerowicz, A., Fraczek, W., Schilling, S., and Alexander, D.: Spatial and temporal distribution of
488 ambient nitric acid and ammonia in the Athabasca Oil Sands Region, Alberta, *J. Limnol.*, 69, 11-21,
489 10.3274/jl10-69-s1-03, 2010.
- 490 Cattell, R. B.: The Scree Test For The Number Of Factors, *Multivariate Behavioral Research*, 1, 245-276,
491 10.1207/s15327906mbr0102_10, 1966.
- 492 Chen, H., Karion, A., Rella, C. W., Winderlich, J., Gerbig, C., Filges, A., Newberger, T., Sweeney, C., and
493 Tans, P. P.: Accurate measurements of carbon monoxide in humid air using the cavity ring-down
494 spectroscopy (CRDS) technique, *Atmos. Meas. Tech.*, 6, 1031-1040, 10.5194/amt-6-1031-2013, 2013.
- 495 National pollutant release inventory (NPRI): [http://open.canada.ca/data/en/dataset/e40099ae-b116-](http://open.canada.ca/data/en/dataset/e40099ae-b116-4c48-9475-f3806fe5a6a6)
496 [4c48-9475-f3806fe5a6a6](http://open.canada.ca/data/en/dataset/e40099ae-b116-4c48-9475-f3806fe5a6a6), access: October 5, 2016, 2013a.
- 497 Measurement instrumentation: carbon dioxide: [https://www.ec.gc.ca/mges-](https://www.ec.gc.ca/mges-ghgm/default.asp?lang=En&n=7903528C-1)
498 [ghgm/default.asp?lang=En&n=7903528C-1](https://www.ec.gc.ca/mges-ghgm/default.asp?lang=En&n=7903528C-1), access: April 25, 2017, 2013b.
- 499 Gorham, E.: Northern peatlands - role in the carbon-cycle and probable responses to climatic warming,
500 *Ecol. Appl.*, 1, 182-195, 10.2307/1941811, 1991.
- 501 Hair, J. F., Anderson, R. E., Tatham, R. L., and Black, W. C.: *Multivariate data analysis*, in, 7th edition ed.,
502 Prentice-Hall, Upper Saddle River, NJ, pp. 108 -110, 1998.
- 503 Holowenko, F. M., MacKinnon, M. D., and Fedorak, P. M.: Methanogens and sulfate-reducing bacteria in
504 oil sands fine tailings waste, *Canadian Journal of Microbiology*, 46, 927-937, 10.1139/cjm-46-10-927,
505 2000.
- 506 Huffman, J. A., Treutlein, B., and Pöschl, U.: Fluorescent biological aerosol particle concentrations and
507 size distributions measured with an Ultraviolet Aerodynamic Particle Sizer (UV-APS) in Central
508 Europe, *Atmos. Chem. Phys.*, 10, 3215-3233, 10.5194/acp-10-3215-2010, 2010.
- 509 Johnson, M. R., Crosland, B. M., McEwen, J. D., Hager, D. B., Armitage, J. R., Karimi-Golpayegani, M., and
510 Picard, D. J.: Estimating fugitive methane emissions from oil sands mining using extractive core
511 samples, *Atmos. Environ.*, 144, 111-123, 10.1016/j.atmosenv.2016.08.073, 2016.
- 512 Liggio, J., Li, S.-M., Hayden, K., Taha, Y. M., Stroud, C., Darlington, A., Drollette, B. D., Gordon, M., Lee, P.,
513 Liu, P., Leithead, A., Moussa, S. G., Wang, D., O'Brien, J., Mittermeier, R. L., Brook, J., Lu, G., Staebler,
514 R., Han, Y., Tokarek, T. W., Osthoff, H. D., Makar, P. A., Zhang, J., Plata, D., and Gentner, D. R.: Oil
515 Sands Operations as a Large Source of Secondary Organic Aerosols, *Nature*, 534, 91-94,
516 10.1038/nature17646, 2016.
- 517 Marey, H. S., Hashisho, Z., Fu, L., and Gille, J.: Spatial and temporal variation in CO over Alberta using
518 measurements from satellites, aircraft, and ground stations, *Atmos. Chem. Phys.*, 15, 3893-3908,
519 10.5194/acp-15-3893-2015, 2015.
- 520 Markovic, M. Z., VandenBoer, T. C., and Murphy, J. G.: Characterization and optimization of an online
521 system for the simultaneous measurement of atmospheric water-soluble constituents in the gas and
522 particle phases, *J. Environ. Monit.*, 14, 1872-1884, 2012.
- 523 Miller, S. M., Worthy, D. E. J., Michalak, A. M., Wofsy, S. C., Kort, E. A., Havice, T. C., Andrews, A. E.,
524 Dlugokencky, E. J., Kaplan, J. O., Levi, P. J., Tian, H. Q., and Zhang, B. W.: Observational constraints on
525 the distribution, seasonality, and environmental predictors of North American boreal methane
526 emissions, *Glob. Biogeochem. Cycle*, 28, 146-160, 10.1002/2013gb004580, 2014.

527 Nara, H., Tanimoto, H., Tohjima, Y., Mukai, H., Nojiri, Y., Katsumata, K., and Rella, C. W.: Effect of air
528 composition (N₂, O₂, Ar, and H₂O) on CO₂ and CH₄ measurement by wavelength-scanned cavity
529 ring-down spectroscopy: calibration and measurement strategy, *Atmos. Meas. Tech.*, 5, 2689-2701,
530 10.5194/amt-5-2689-2012, 2012.

531 Detailed facility information: [http://www.ec.gc.ca/inrp-npri/donnees-](http://www.ec.gc.ca/inrp-npri/donnees-data/index.cfm?do=facility_information&lang=En&opt_npri_id=0000002274&opt_report_year=2013)
532 [data/index.cfm?do=facility_information&lang=En&opt_npri_id=0000002274&opt_report_year=2013](http://www.ec.gc.ca/inrp-npri/donnees-data/index.cfm?do=facility_information&lang=En&opt_npri_id=0000002274&opt_report_year=2013)
533 , access: April 13, 2017, 2013.

534 Nwaishi, F., Petrone, R. M., Macrae, M. L., Price, J. S., Strack, M., and Andersen, R.: Preliminary
535 assessment of greenhouse gas emissions from a constructed fen on post-mining landscape in the
536 Athabasca oil sands region, Alberta, Canada, *Ecol. Eng.*, 95, 119-128, 10.1016/j.ecoleng.2016.06.061,
537 2016.

538 Odame-Ankrah, C. A.: Improved detection instrument for nitrogen oxide species, Ph.D., Chemistry,
539 University of Calgary, <http://hdl.handle.net/11023/2006>, Calgary, 2015.

540 Oertel, C., Matschullat, J., Zurba, K., Zimmermann, F., and Erasmi, S.: Greenhouse gas emissions from
541 soils A review, *Chem Erde-Geochem.*, 76, 327-352, 10.1016/j.chemer.2016.04.002, 2016.

542 Onasch, T. B., Trimborn, A., Fortner, E. C., Jayne, J. T., Kok, G. L., Williams, L. R., Davidovits, P., and
543 Worsnop, D. R.: Soot Particle Aerosol Mass Spectrometer: Development, Validation, and Initial
544 Application, *Aerosol Sci. Technol.*, 46, 804-817, 10.1080/02786826.2012.663948, 2012.

545 Percy, K. E.: Ambient Air Quality and Linkage to Ecosystems in the Athabasca Oil Sands, Alberta, *Geosci.*
546 *Can.*, 40, 182-201, 2013.

547 Phillips-Smith, C., Jeong, C. H., Healy, R. M., Dabek-Zlotorzynska, E., Celio, V., Brook, J. R., and Evans, G.:
548 Sources of Particulate Matter in the Athabasca Oil Sands Region: Investigation through a Comparison
549 of Trace Element Measurement Methodologies, *Atmos. Chem. Phys. Discuss.*, 2017, 1-34,
550 10.5194/acp-2016-966, 2017.

551 Quagraine, E. K., Headley, J. V., and Peterson, H. G.: Is biodegradation of bitumen a source of recalcitrant
552 naphthenic acid mixtures in oil sands tailing pond waters?, *J. Environ. Sci. Health Part A-Toxic/Hazard.*
553 *Subst. Environ. Eng.*, 40, 671-684, 10.1081/ese-200046637, 2005.

554 Rooney, R. C., Bayley, S. E., and Schindler, D. W.: Oil sands mining and reclamation cause massive loss of
555 peatland and stored carbon, *Proc. Natl. Acad. Sci. U.S.A.*, 109, 4933-4937, 10.1073/pnas.1117693108,
556 2012.

557 Shephard, M. W., McLinden, C. A., Cady-Pereira, K. E., Luo, M., Moussa, S. G., Leithead, A., Liggio, J.,
558 Staebler, R. M., Akingunola, A., Makar, P., Lehr, P., Zhang, J., Henze, D. K., Millet, D. B., Bash, J. O.,
559 Zhu, L., Wells, K. C., Capps, S. L., Chaliyakunnel, S., Gordon, M., Hayden, K., Brook, J. R., Wolde, M.,
560 and Li, S. M.: Tropospheric Emission Spectrometer (TES) satellite observations of ammonia,
561 methanol, formic acid, and carbon monoxide over the Canadian oil sands: validation and model
562 evaluation, *Atmospheric Measurement Techniques*, 8, 5189-5211, 10.5194/amt-8-5189-2015, 2015.

563 Small, C. C., Cho, S., Hashisho, Z., and Ulrich, A. C.: Emissions from oil sands tailings ponds: Review of
564 tailings pond parameters and emission estimates, *Journal of Petroleum Science and Engineering*, 127,
565 490-501, 10.1016/j.petrol.2014.11.020, 2015.

566 Thompson, R. L., Sasakawa, M., Machida, T., Aalto, T., Worthy, D., Lavric, J. V., Myhre, C. L., and Stohl, A.:
567 Methane fluxes in the high northern latitudes for 2005-2013 estimated using a Bayesian atmospheric
568 inversion, *Atmos. Chem. Phys.*, 17, 3553-3572, 10.5194/acp-17-3553-2017, 2017.

569 Tokarek, T. W., Huo, J. A., Odame-Ankrah, C. A., Hammoud, D., Taha, Y. M., and Osthoff, H. D.: A gas
570 chromatograph for quantification of peroxy-carboxylic nitric anhydrides calibrated by thermal
571 dissociation cavity ring-down spectroscopy, *Atmos. Meas. Tech.*, 7, 3263-3283, 10.5194/amt-7-3263-
572 2014, 2014.

573 Tokarek, T. W., Brownsey, D. K., Jordan, N., Garner, N. M., Ye, C. Z., Assad, F. V., Peace, A., Schiller, C. L.,
574 Mason, R. H., Vingarzan, R., and Osthoff, H. D.: Biogenic Emissions and Nocturnal Ozone Depletion

575 Events at the Amphitrite Point Observatory on Vancouver Island, Atmosphere-Ocean, 1-12,
576 10.1080/07055900.2017.1306687, 2017.

577 Wang, X. L., Chow, J. C., Kohl, S. D., Percy, K. E., Legge, A. H., and Watson, J. G.: Characterization of
578 PM_{2.5} and PM₁₀ fugitive dust source profiles in the Athabasca Oil Sands Region, J. Air Waste Manag.
579 Assoc., 65, 1421-1433, 10.1080/10962247.2015.1100693, 2015.

580 Warner, D. L., Villarreal, S., McWilliams, K., Inamdar, S., and Vargas, R.: Carbon Dioxide and Methane
581 Fluxes From Tree Stems, Coarse Woody Debris, and Soils in an Upland Temperate Forest, Ecosystems,
582 10.1007/s10021-016-0106-8, 2017.

583 Warren, L. A., Kendra, K. E., Brady, A. L., and Slater, G. F.: Sulfur Biogeochemistry of an Oil Sands
584 Composite Tailings Deposit, Front. Microbiol., 6, 14, 10.3389/fmicb.2015.01533, 2016.

585 Wesely, M. L., and Hicks, B. B.: A review of the current status of knowledge on dry deposition, Atmos.
586 Environm., 34, 2261-2282, 10.1016/S1352-2310(99)00467-7, 2000.

587 Whalen, S. C.: Biogeochemistry of methane exchange between natural wetlands and the atmosphere,
588 Environ. Eng. Sci., 22, 73-94, 10.1089/ees.2005.22.73, 2005.

589 Whaley, C., Makar, P. A., Shephard, M. W., Zhang, L., Zhang, J., Zheng, Q., Akingunola, A., Wentworth, G.
590 R., Murphy, J. G., Kharol, S. K., and Cady-Pereira, K. E.: Contributions of natural and anthropogenic
591 sources to ambient ammonia in the Athabasca Oil Sands and north-western Canada, Atmos. Chem.
592 Phys., submitted, 2017.

593 Wilson, N. K., Barbour, R. K., Chuang, J. C., and Mukund, R.: Evaluation of a real-time monitor for fine
594 particle-bound PAH in air, Polycycl. Aromat. Compd., 5, 167-174, 10.1080/10406639408015168,
595 1994.

596 Yavitt, J. B., Williams, C. J., and Wieder, R. K.: Soil chemistry versus environmental controls on
597 production of CH₄ and CO₂ in northern peatlands, Eur. J. Soil Sci., 56, 169-178, 10.1111/j.1365-
598 2389.2004.00657.x, 2005.

599 Zhang, L. M., Brook, J. R., and Vet, R.: On ozone dry deposition - with emphasis on non-stomatal uptake
600 and wet canopies, Atmos. Environm., 36, 4787-4799, 10.1016/s1352-2310(02)00567-8, 2002.

601

602